Research Article Vol. 59, No. 13 / 1 May 2020 / Applied Optics D59

applied optics

Hopkins procedure for tunable magnification: surgical spectacles

Cristina M. Gómez-Sarabia[1] and Jorge Ojeda-Castañeda[2,*]

[1]Departamento de Artes Digitales, Universidad de Guanajuato, Salamanca, Guanajuato 36885, México, Mexico
[2]Departamento de Electrónica, Universidad de Guanajuato, Salamanca, Guanajuato 36885, México, Mexico
*Corresponding author: jojedacas@ugto.mx

Received 4 December 2019; revised 30 January 2020; accepted 30 January 2020; posted 31 January 2020 (Doc. ID 385044); published 27 February 2020

We analyze the use of two varifocal lenses, with fixed interlens separation, for achieving tunable magnification at a specific throw. Our discussion extends the Hopkins procedure circumscribed to the determination of fixed optical powers in a multilens system. We illustrate our results by presenting the Gaussian optics design of surgical spectacles, which have tunable magnification while generating virtual images with zero throw. We also report novel formulas describing this type of two-lens zoom system, which works without any mechanical compensation. © 2020 Optical Society of America

https://doi.org/10.1364/AO.385044

1. INTRODUCTION

Presently, there are several competing technologies for implementing varifocal lenses [1–5]. Independently of the winning technology, there is a parallel trend for designing novel optical systems employing varifocal lenses [6–9].

Kitajima is credited for designing the first varifocal lens [10,11]. Lohmann [12–15] and Alvarez [16], independently and simultaneously, proposed a novel method for setting varifocal lenses by using a pair of cubic phase masks, which are lateral displaced.

Related to the Lohmann–Alvarez proposal, it is now known that, by in-plane rotating a pair of diffractive lenses [17,18] or by rotating a pair of refractive masks [19–21], one can also implement varifocal lenses.

On the other hand, in a seminal paper, Hopkins discussed the generic formula for designing optical systems with multielements [22]. Application of the Hopkins procedure has a quite significant record [23–32].

To our knowledge, the Hopkins procedure considers only the use of elements with fixed optical power. In what follows, we extend the Hopkins procedure for employing two varifocal lenses that work at fixed interlens separation while generating tunable magnification with fixed throw.

For illustrating our proposal, we present the Gaussian optics of tunable magnification spectacles [33], which employs two varifocal lenses with fixed interlens separation. For emphasizing the tuneability of our proposal, we explore numerically the impact on optical powers, when changing the lateral magnification in the range $1.2 \leq M \leq 5$. Inside this range, we find that the optical powers have achievable values.

For the sake of clarity in our discussion, in Section 2 we discuss the use of two varifocal lenses for tuning the magnification of virtual images, at zero throw. In Section 3, we report new formulas describing the variable optical powers, of the composing elements, as well as the equivalent optical power. In Section 4, we present the formula specifying the positions of the principal planes and those of the focal planes. In Section 5, we summarize our contribution.

2. TUNABLE MAGNIFICATION WITH ZERO THROW

In Fig. 1(a) we show a 3D diagram of a two-lens system, which reduces angular magnification, with zero throw. Equivalently, the axial object point and the axial image plane are Bravais points [34]. In Fig. 1(b), we depict the main paraxial variables for describing the optical system.

As indicated in Fig. 1, we denote as $z_0 < 0$ the reduced distance between the object plane and the first lens. Because the reduced interlens separation is $d > 0$, the reduced distance from the second lens to the image plane is equal to $z_0 - d < 0$. Consequently, if we denote as $y_1 > 0$ the height of the paraxial ray (in red) at the first element, then the incident paraxial angle is

$$n_0 \, u_0 = -\frac{y_1}{z_0} > 0. \tag{1}$$

In Eq. (1) we denote as n_0 the refractive index of the space located between the input plane and the first lens. At the second element, the height of the paraxial ray is denoted as y_2. We note that, after the second element, the paraxial angle is

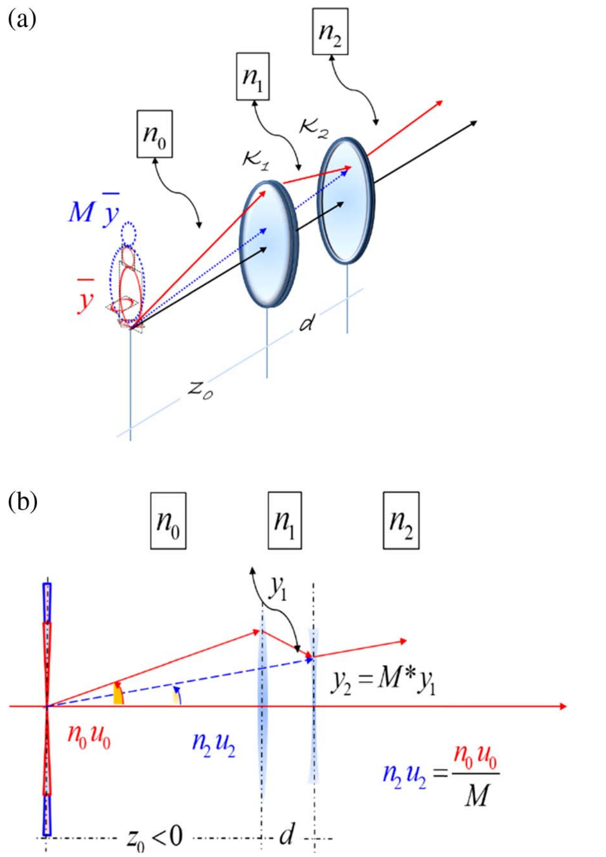

Fig. 1. Schematics of the Gaussian design. (a) Angular reduction of the paraxial marginal ray (in red). (b) Relevant variables. The refractive indices are specified inside boxes.

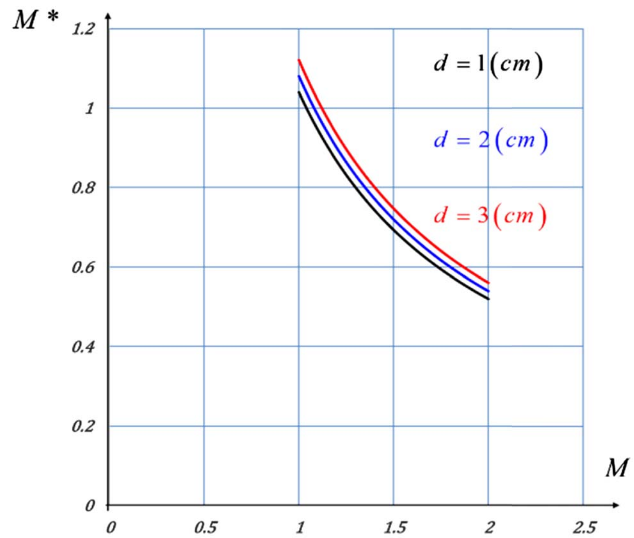

Fig. 2. Hyperbolas depicting the relationship between the magnification and the height ratio, as in Eq. (5), for $z_0 = -25$ (cm) and for three values of interlens separation: $d = 1$ (cm), 2 (cm), and $d = 3$ (cm).

$$n_2\, u_2 = -\frac{y_2}{(z_0 - d)} > 0. \tag{2}$$

In Eq. (2) we denote as n_2 the refractive index after the interlens separation. Now it is convenient to denote the ratio between the two paraxial heights as

$$M^* = \frac{y_2}{y_1}. \tag{3}$$

Next, we recognize that the lateral magnification is

$$M = \frac{n_0\, u_0}{n_2\, u_2} > 1. \tag{4}$$

Then, by substituting Eqs. (1)–(3) in Eq. (4), we have that

$$M\, M^* = 1 - \frac{d}{z_0}. \tag{5}$$

For our current discussion, we have employed $z_0 = -25$ (cm), which is apparently a good working distance for a surgeon. This value is also useful for making comparisons between our numerical simulations and the results reported by Mouroulis and Macdonald, who set $z_0 = -25$ (cm) and $d = 3$ (cm). (See [33].)

In Fig. 2 we plot the relationship in Eq. (5) for three different values of the reduced interlens separation d and for $z_0 = -25$ (cm). It is apparent from Fig. 2 that the height ratios do not change substantially if the values of interlens separation are in the range (1 cm, 3 cm). For our current discussion, we set $d = 3$ (cm). Our choice is useful for making comparisons with the results in [33].

3. OPTICAL POWERS WITH TUNABLE MAGNIFICATION

Next, we follow the procedure outlined by Hopkins, in [22], for obtaining the optical power of the first element

$$K_1 = -\frac{1}{z_0} + \frac{1 - M^*}{d}. \tag{6}$$

By employing the expression of M^*, in Eq. (5), we can rewrite the required optical power in Eq. (6), as a function of the lateral magnification

$$K_1 = \left(\frac{1}{d}\right)\left(1 - \frac{1}{M}\right)\left(1 - \frac{d}{z_0}\right). \tag{7}$$

To our current knowledge, Eq. (9) is a novel formula. Next, we proceed in a similar fashion, for obtaining the optical power of the second element. According to the Hopkins procedure, we have that

$$K_2 = -\left(\frac{1}{d}\right)\left(\frac{1}{M^*} - \frac{1}{1 - \frac{d}{z_0}}\right). \tag{8}$$

Next, by substituting the value of M^* (as a function of M) in Eq. (8), we obtain

$$K_2 = -\left(\frac{1}{d}\right)\frac{(M-1)}{\left(1 - \frac{d}{z_0}\right)}. \tag{9}$$

Again, to our current knowledge, Eq. (9) is a novel formula. The result in Eq. (9) specifies the optical power of the second element, as a function of the lateral magnification.

Next, we use Eqs. (7) and (9) for obtaining the equivalent optical power, which reads

$$K = \left(-\frac{1}{z_0}\right)\left(1-\frac{1}{M}\right)\frac{\left(M+1-\frac{d}{z_0}\right)}{\left(1-\frac{d}{z_0}\right)}. \tag{10}$$

In Fig. 3(a), we plot the variations of K_1, K_2, and K as functions of the lateral magnification M. The curves consider that the interlens separation can have three different values: $d = 1$ (cm), 2 (cm), and $d = 3$ (cm), while as before $z_0 = -25$ (cm). It is apparent from Fig. 3(a) that the equivalent optical power varies slowly with changes of the interlens separation.

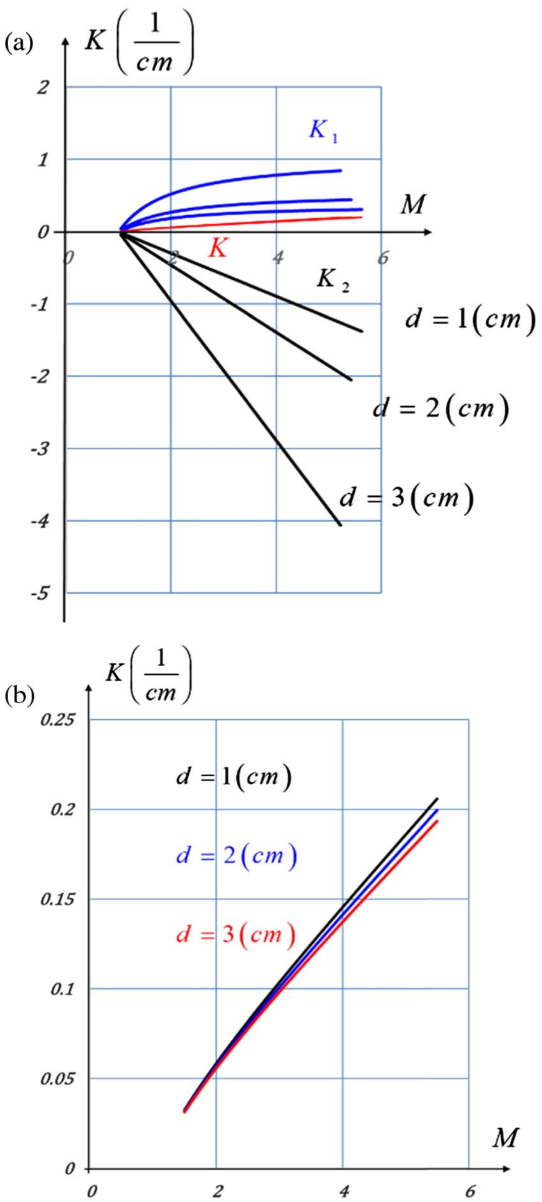

Fig. 3. Variations of the optical powers, K_1, K_2, and K, as a function of the lateral magnification. (a) Plot of optical power variations for three different values of the interlens separation d = 1 (cm), 2 (cm), and d = 3 (cm). (b) Plot of variations of the equivalent optical power at a different scale.

For a close look at this situation, in Fig. 3(b), we plot at a different scale Eq. (10). This later graph verifies that the equivalent optical power varies slowly as one modifies the interlens separation.

Here, it is relevant to indicate that, in Fig. 3, we employ units of 1/cm, for plotting, along the vertical axis, the values of optical power.

4. PRINCIPAL PLANES AND FOCAL PLANES

We remember that, for optical systems that have elements with fixed optical powers, the positions of the principal planes remain at constant locations. However, if the elements have variable optical powers, then positions of the principal planes vary as the magnification changes.

In what follows, we report new formulas, as well as the graphs, that describe the variations of the back focal distance, f_{Back}; the front focal distance, f_{Front}; the distance from the first element to the front-principal plane, δH; and the distance from the second element to the back-principal plane, $\delta H'$.

As depicted in Fig. 4(a), to our end, we trace a paraxial ray that impinges the first element, with an angle equal to zero. After the first refraction, the paraxial ray hits the second element, with a height $y_2 = M_{-\infty}\, y_1$; where now the height ratio $M_{-\infty}$ is

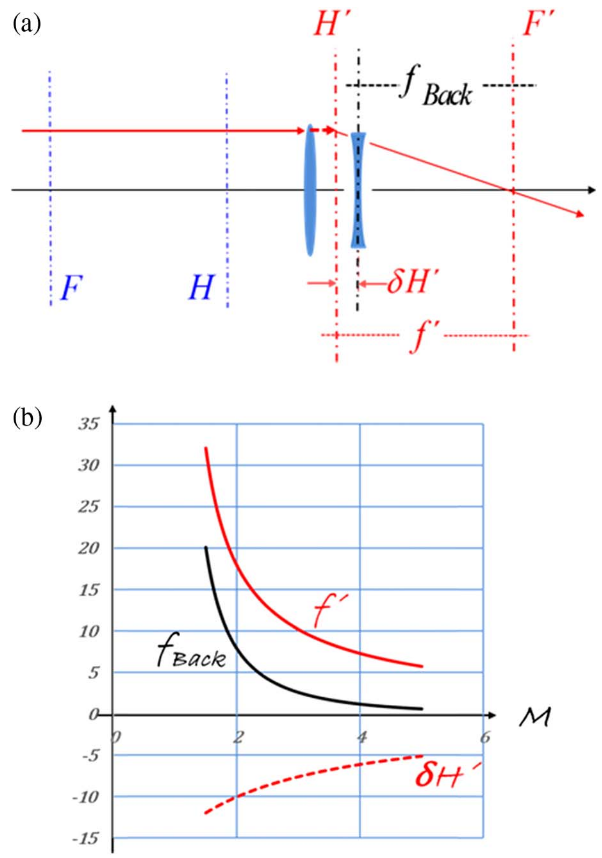

Fig. 4. Back cardinal planes. (a) Schematic depicting the back-principal plane H' and the back focal plane F'. (b) As a function of the lateral magnification, we plot the variations of the focal length, f', the back focal distance f_{Back}, and the position of the back-principal plane, $\delta H'$.

$$M_{-\infty} = \frac{d}{z_0} + \frac{1}{M}\left(1 - \frac{d}{z_0}\right). \quad \textbf{(11)}$$

To our knowledge, Eq. (11) is a novel formula.

After the second refraction, the paraxial ray intercepts the optical axis at the back focal point. Hence, the back focal length is

$$f_{\text{Back}} = -\left(\frac{1-\frac{d}{z_0}}{M-1}\right)\left(\frac{1+(M-1)\frac{d}{z_0}}{M+1-\frac{d}{z_0}}\right) z_0. \quad \textbf{(12)}$$

To our knowledge, Eq. (12) is a novel formula.

Because the focal length can be expressed as $f' = f_{\text{Back}} - \delta H'$, the distance from the second element to the back-principal plane is

$$\delta H' = -\frac{K_1}{K} d = \frac{\left(1-\frac{d}{z_0}\right)^2}{M+1-\frac{d}{z_0}} z_0. \quad \textbf{(13)}$$

In Fig. 4(b), we note that, as M increases, the values of f', f_{Back}, and $\delta H'$ tend to zero.

Next, as depicted in Fig. 5(a), we consider a paraxial ray that leaves the optical system with a paraxial angle equal to zero.

This condition can be rephased as follows. We trace backward the exit ray, in blue. Then, the ray in blue impinges on the second element with an angle equal to zero.

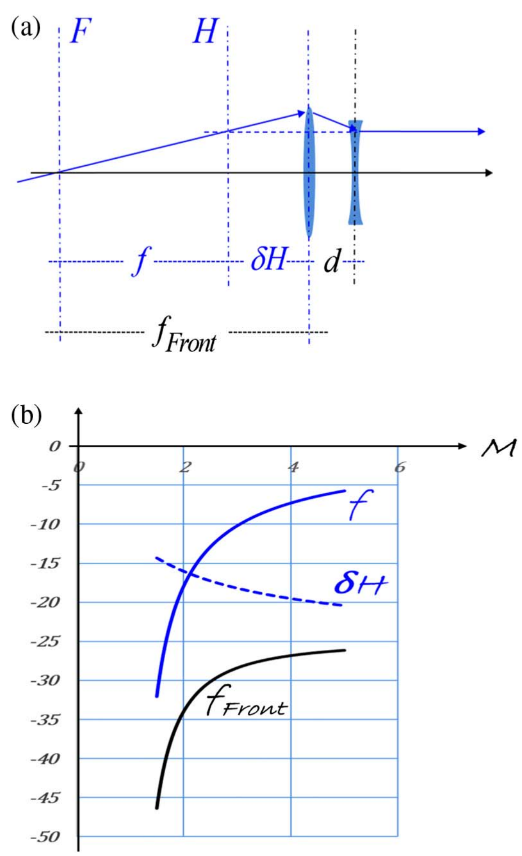

Fig. 5. Front cardinal planes. (a) Schematic depicting the focal plane F and the front-principal plane H. (b) Variations of the front focal distance f_{Front} as well as changes of the distance between the first optical element to the front-principal plane δH.

After a refraction at the second element, the ray hits the first element with a height $y_2 = M_\infty y_1$, where the height ratio M_∞ is

$$M_\infty = \frac{M - \frac{d}{z_0}}{1 - \frac{d}{z_0}}. \quad \textbf{(14)}$$

To our knowledge, Eq. (14) is a novel formula.

Next, after the refracting at the first element, the ray intercepts the optical axis at the front focal point. Hence, the front focal length is

$$f_{\text{Front}} = \left(\frac{M z_0}{M+1-\frac{d}{z_0}}\right)\left(\frac{M-\frac{d}{z_0}}{1-\frac{d}{z_0}}\right). \quad \textbf{(15)}$$

Because the front focal length is $f = f_{\text{Front}} - \delta H$, the distance from the first element to the front-principal plane is

$$\delta H = \frac{K_2}{K} d = \frac{\left(1-\frac{d}{z_0}\right)}{M+1-\frac{d}{z_0}} z_0. \quad \textbf{(16)}$$

To our knowledge, Eq. (16) is a novel formula.

The separation between the principal planes is

$$\Delta H = d + \delta H' - \delta H. \quad \textbf{(17)}$$

By substituting the results in Eqs. (13) and (16), we can rewrite Eq. (17) as

$$\Delta H = -\frac{(M-1)(1-\frac{d}{z_0})}{\left[M+1-\frac{d}{z_0}\right]} z_0. \quad \textbf{(18)}$$

To our knowledge, Eq. (18) is a novel formula.

In Fig. 6, we display the values of δH, $\delta H'$, and ΔH as functions of the lateral magnification M.

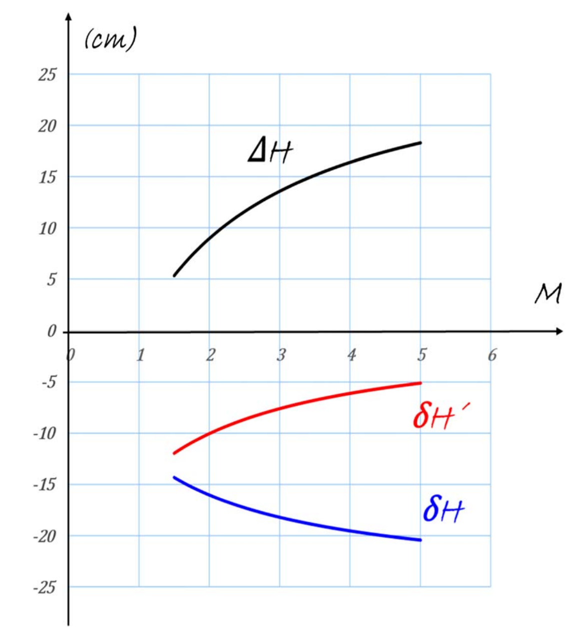

Fig. 6. Principal plane locations and the separation between the principal planes.

As pointed out in the introduction, our numerical evaluations show that, when changing the lateral magnification, in the range $1.2 \leq M \leq 5$, the optical powers have achievable values.

5. FINAL REMARKS

We have presented an analysis on the use of two varifocal lenses for achieving tunable magnification between conjugate planes.

We have considered that the optical system has a fixed inter-lens separation and a prespecified throw. As the magnification changes, there is no need of any mechanical compensation.

Our current analysis extends the seminal Hopkins procedure, which is circumscribed to the specification of fixed optical powers, in a multilens system.

For illustrating our proposal, we have presented a first-order design of surgical spectacles, which have tunable magnification while generating virtual images with zero throw. If you will, with variable magnification, an axial object plane and its conjugate image remain at the same location as Bravais points.

By explicitly incorporating as a variable the tunable magnification, we have reported novel formulas [Eqs. (7), (8), and (10)], which explicitly express the variation of the optical powers as a function of the tunable magnification.

We have also unveiled formulas that describe, as a function of the changing magnification, the locations of the principal planes, δH and $\delta H'$, as well as the values of the front focal length and of the back focal length. To the best of our knowledge, these relationships are new.

Disclosures. The authors declare no conflicts of interest related to this paper.

REFERENCES

1. B. Berge and J. Peseux, "Variable focal lens controlled by an external voltage: an application of electrowetting," Eur. Phys. J. E **3**, 159–163 (2000).
2. H. W. Ren, Y. H. Fan, S. Gauza, and S. T. Wu, "Tunable-focus flat liquid crystal spherical lens," Appl. Phys. Lett. **84**, 4789–4791 (2004).
3. T. Martinez, D. V. Wick, D. M. Payne, J. T. Baker, and S. R. Restaino, "Non-mechanical zoom system," Proc. SPIE **5234**, 375–378 (2004).
4. D. Y. Zhang, N. Justis, and Y. H. Lo, "Fluidic adaptive zoom lens with high zoom ratio and widely tunable field of view," Opt. Commun. **249**, 175–182 (2005).
5. B. H. W. Hendriks, S. Kuiper, M. A. J. Van As, C. A. Renders, and T. W. Tukker, "Electrowetting-based variable-focus lens for miniature systems," Opt. Rev. **12**, 255–259 (2005).
6. J. Schwiegerling and C. Paleta-Toxqui, "Minimal movement zoom lens," Appl. Opt. **48**, 1932–1935 (2009).
7. A. Mikš and J. Novák, "Analysis of two-element zoom systems based on variable power lenses," Opt. Express **18**, 6797–6810 (2010).
8. A. Mikš and J. Novák, "Three-component double conjugate zoom lens system from tunable focus lenses," Appl. Opt. **52**, 862–865 (2013).
9. A. Mikš and J. Novák, "Paraxial imaging properties of double conjugate zoom lens system composed of three tunable-focus lenses," Opt. Lasers Eng. **53**, 86–89 (2014).
10. W. T. Plummer, J. G. Baker, and J. van Tassell, "Photographic optical systems with nonrotational aspheric surfaces," Appl. Opt. **38**, 3572–3592 (1999).
11. I. Kitajima, "Improvements in lenses," British Patent 250,268 (July 29, 1926).
12. A. W. Lohmann, "Lentille de distance focale variable," French Patent 1,398,35 (June 10, 1964).
13. A. W. Lohmann, "Lente focale variabile," Italian Patent 727,848 (June 19, 1964).
14. A. W. Lohmann, "Improvements relating to lenses and to variable optical lens systems formed by such lenses," London Patent Specification 998,191 (29 May 1964).
15. A. W. Lohmann, "A new class of varifocal lenses," Appl. Opt. **9**, 1669–1671 (1970).
16. L. W. Alvarez, "Two-element variable-power spherical lens," U.S.patent 3,305,294 (3 December 1964).
17. J. Ojeda-Castaneda, J. E. A. Landgrave, and C. M. Gómez-Sarabia, "Conjugate phase plate use in analysis of the frequency response of optical systems designed for extended depth of field," Appl. Opt. **47**, E99–E105 (2008).
18. J. Ojeda-Castaneda, E. Aguilera Gómez, H. P. Mora, M. T. Cisneros, E. R. L. Orozco, A. L. Martínez, J. S. P. Santamaría, J. G. M. Castro, and R. C. S. Segoviano, "Optical system with variable field depth," U.S. patent 8,159,573 (17 April 2012).
19. J. Ojeda-Castaneda, S. Ledesma, and C. M. Gómez-Sarabia, "Tunable apodizers and tunable focalizers using helical pairs," Photon. Lett. Poland **5**, 20–22 (2013).
20. A. Grewe, P. Fesser, and S. Sinzinger, "Diffractive array optics tuned by rotation," Appl. Opt. **56**, A89–A96 (2017).
21. S. Bernet, "Zoomable telescope by rotation of toroidal lenses," Appl. Opt. **57**, 8087–8095 (2018).
22. H. H. Hopkins, "The gaussian optics of multilens systems," in *Proceedings Conference on Optical Instruments and Techniques* (Chapman & Hall, 1961), pp. 133–159.
23. T. Kryszczynski, "Paraxial determination of the general four component zoom system with mechanical compensation," Proc. SPIE **2539**, 180–191 (1995).
24. L. Hazra, "Structural design of multicomponent lens systems," Appl. Opt. **23**, 4440–4443 (1984).
25. D. V. Wick and T. Martinez, "Adaptive optical zoom," Opt. Eng. **43**, 8–9 (2004).
26. X. Cheng, Y. Wang, Q. Hao, and J. M. Sasian, "Expert system for generating initial layout of zoom systems with multiple moving lens group," Opt. Eng. **44**, 1–8 (2005).
27. L. N. Hazra and S. Pal, "A novel approach for structural synthesis of zoom systems," Proc. SPIE **7786**, 778607-1–11 (2010).
28. S. Pal and L. N. Hazra, "Stabilization of pupils in a zoom lens with two independent movements," Appl. Opt. **52**, 5611–5618 (2013).
29. S. Pal, "Aberration correction of zoom lenses using evolutionary programming," Appl. Opt. **52**, 5724–5732 (2013).
30. J. Ojeda-Castaneda, C. M. Gómez-Sarabia, and S. Ledesma, "Novel zoom systems using a vortex pair," Asian J. Phys. **23**, 415–424 (2014).
31. J. Ojeda-Castaneda, C. M. Gómez-Sarabia, and S. Ledesma, "Compact telephoto objectives with zero Petzval sum using varifocal lenses," Asian J. Phys. **23**, 535–542 (2014).
32. J. Ojeda-Castaneda and C. M. Gómez-Sarabia, "Nonconventional optical systems using varifocal lenses," Photon. Lett. Poland **7**, 14–16 (2015).
33. P. Mouroulis and J. Macdonald, *Geometrical Optics and Optical Design* (Oxford University, 1997), pp. 270–289.
34. R. S. Longhurst, *Geometrical and Physical Optics* (Longman, 1970), p. 38.